Hindawi
Mathematical Problems in Engineering
Volume 2021, Article ID 6338625, 14 pages
https://doi.org/10.1155/2021/6338625

Research Article

Influence of Pitch Error on Vibration, Bifurcation, and Chaos Characteristics of the Helical Gear Pair System

Shijie Pan, Youtang Li, and Juane Wang

School of Mechanical and Electronical Engineering, Lanzhou University of Technology, Lanzhou 730050, China

Correspondence should be addressed to Shijie Pan; 15809313125@163.com and Youtang Li; liyt@lut.cn

Received 22 August 2021; Accepted 15 October 2021; Published 11 November 2021

Academic Editor: Zenghui Wang

Aiming at the problem of pitch error of helical gear pair in engineering practice, the influence of pitch error on vibration, bifurcation, and chaos characteristics of the helical gear pair system is mainly studied. Due to the periodic time-varying nature of pitch error, a method of simulating the pitch error as a sine function is proposed to calculate pitch error. A nonlinear dynamic model of bending-torsion-shaft coupling of the helical gear pair system is established considering the effect of pitch error. The influence of pitch error on the vibration, bifurcation, and chaos characteristics of the system is analyzed by the Runge–Kutta numerical integration method. The research results show that the introduction of pitch error has the most significant impact on the torsional vibration of the system. With the increase in pitch error, the system exhibits rich bifurcation and chaos characteristics in the torsional direction. Moreover, it is also found that the vibration response in the torsional orientation of the system increases or decreases to the same degree when the system is in a periodic motion state, and the pitch error varies by the same extent. Therefore, the impact of pitch error on the dynamic performance of the helical gear pair system should be considered in engineering practice.

1. Introduction

Helical gear pairs are widely used in various machines and mechanical equipment. They are one of the most crucial motion and power transmission devices, whose mechanical properties have an important influence on the whole machine's vibration, noise, and reliability. Due to the constraints of the actual engineering conditions, there are inevitable meshing errors in the operation of gear pairs. As the most critical component of gear meshing error, pitch error significantly impacts the dynamic characteristics of gear transmission systems. Therefore, it is vital to study the effect of pitch error on the vibration, bifurcation, and chaos characteristics of gear transmission systems.

In recent years, many scholars have conducted a lot of research on the nonlinear dynamics of gear systems. Yang et al. [1] established a nonlinear dynamics model of the helical gear system considering tooth wear and analyzed the effect of tooth wear on the bifurcation and chaos characteristics of the system. References [2, 3] discussed in detail the bifurcation and chaos and other nonlinear dynamic characteristics of the multibody mechanical systems with revolute clearance joint and imperfect joint. Wang et al. [4] developed a finite element model of a helical gear rotor system considering the effect of time-varying meshing stiffness and investigated the effect of different coupling forms and helix angles on the vibration characteristics of the system. In literatures [5–10], the effects of tooth surface friction, meshing misalignment, meshing impact, tooth side clearance, and geometric eccentricity on the vibration characteristics of helical gear systems were investigated. Han and Qi [11] studied the influence of tooth spalling and local fracture on the meshing stiffness and vibration characteristics of the helical gear pair system. Huang et al. [12] studied the effects of excitation frequency, backlash, meshing damping ratio, and bearing radial clearance on bifurcation and chaos characteristics of the high contact ratio gear system. Zhang et al. [13] investigated the impact of bearing clearance on the vibration characteristics of the spur gear transmission system. Xu et al. [14] established a

mathematical model of spur gear tooth surface including tooth profile deviation and analyzed the influence of different tooth profile deviations on transmission error and dynamic characteristics of the system. Arian and Taghvaei [15] developed a nonlinear dynamics model of a spur gear transmission system with an idler and analyzed the effect of the idler on the chaotic characteristics of the system and the control of system chaos. Saghafi and Farshidianfar [16] proposed a control system for the elimination of chaotic behaviors in spur gear systems and verified the effectiveness of the proposed control system in eliminating homoclinic bifurcation and chaos in nonlinear gear systems. Hua and Chen [17] developed a finite element dynamics model of the bevel gear transmission system considering bearing elasticity and analyzed the effect of bearing elasticity on the vibration characteristics of the system. Yin et al. [18] researched the influence of oil film among meshing teeth on vibration characteristics of the herringbone gear transmission system. Li et al. [19] conducted a global dynamics analysis of a mechanical model with three nonsmooth factors, namely, elastic impact, rigid impact, and dry friction, and comprehensively discussed the effects of different nonsmooth factors on the system motions distribution and transition. Makarenkov and Lamb [20] discussed in detail the research directions in the dynamics of nonsmooth systems and the related bifurcation theories such as border-collision bifurcation and grazing bifurcation. References [21, 22] studied in detail the bifurcation and chaos and other nonlinear dynamic characteristics of the nonsmooth dynamic systems based on the OGY state feedback control law with the help of bifurcation diagrams such as border-collision bifurcation and torus bifurcation.

Moreover, in the process of nonlinear dynamic analysis of gear systems, the gear pitch error problem has always been a research hotspot. Umezawa et al. [23, 24] built a pure torsional nonlinear dynamics model of the spur gear system and analyzed the effects of pressure angle and pitch error on the vibration characteristics of the system. Liu et al. [25] built a nonlinear dynamics model of a spur gear pair system considering pitch deviation under multistate meshing conditions and investigated the effects of operating parameters and system parameters on the nonlinear dynamic characteristics of the system under multistate meshing conditions. Handschuh et al. [26] studied the influence of pitch error on tooth root stress of the spur gear pair system. In literatures [27–29], the impact of pitch error on the dynamic transmission error and vibration characteristics of the spur gear pair system was investigated by means of numerical simulations and experiments. Franulovic et al. [30] studied the influence of pitch error on load distribution of contact teeth of the high contact ratio spur gear transmission system. References [31–33] founded the nonlinear dynamic model of the two-stage spur gear transmission system and researched the impact of backlash and pitch error on the vibration and chaos characteristics of the system. Chen and Tang [34] studied the effect of pitch error on the vibration characteristics of the herringbone gear system. References [35–37] investigated the influence of pitch error on meshing stiffness and vibration noise of the cylindrical helical gear transmission system. Guo and Fang [38] proposed a new method to calculate the meshing impact based on the measured pitch error and analyzed the effect of the meshing impact on the vibration and chaos characteristics of the helical gear transmission system. The above literature mainly studies the effect of pitch error on the dynamic characteristics of spur gear systems. However, there are not many articles that consider the impact of pitch error on the dynamic characteristics of helical gear systems and analyze the vibration, bifurcation, and chaos characteristics of helical gear systems.

Therefore, this paper comprehensively considers the pitch error, time-varying meshing stiffness, meshing damping, and tooth side clearance and establishes the bending-torsion-shaft coupling nonlinear dynamic model of the helical gear pair system. Through the numerical analysis of the dynamic model, combined with the time-domain diagrams, spectrum maps, phase diagrams, Poincaré cross-section graphs, bifurcation diagram, and largest Lyapunov exponent (LLE) chart of the system response, the influence of pitch error on the vibration, bifurcation, and chaos characteristics of the helical gear pair system is studied in detail. The research results can provide theoretical support for analyzing vibration, bifurcation, and chaos characteristics of the helical gear pair system with pitch errors.

The structure of this paper is organized as follows: the nonlinear dynamic model and equations of motion of the system are established in Section 2, where the pitch error, time-varying meshing stiffness, meshing damping, and tooth side clearance of the system are given. In Section 3, the equations of motion of the system are solved by the numerical integral method, and then the effect of pitch error on the vibration, bifurcation, and chaos characteristics of the system is investigated. Ultimately, some brief conclusions are given in Section 4.

2. The Nonlinear Dynamic Model of Helical Gear Pair considering Pitch Error

Comprehensively considering the pitch error, time-varying meshing stiffness, meshing damping, tooth side clearance, and other nonlinear factors, a six degree of freedom bending-torsion-shaft coupling nonlinear dynamic model of the helical gear pair system with pitch error is established using the lumped mass method [39] as shown in Figure 1. Ignoring the effect of friction between gear teeth, only the torsional vibration of the driving and driven gear around the z-axis, the axial vibration of the driving and driven gear along the z-axis, and the transverse bending vibration of the driving and driven gear along the y-axis are considered. In this model, m_p and m_g represent the mass of the driving and driven gears, respectively; I_p and I_g represent the moment of inertia; r_{bp} and r_{bg} represent the radius of the base circle; k_{pz} and k_{gz} represent the equivalent bearing support stiffness of the driving and driven gears in the axial direction (z-direction), respectively; k_{py} and k_{gy} represent the equivalent bearing support stiffness in the tangential direction (y-direction); c_{pz} and c_{gz} represent the equivalent damping in the axial direction; c_{py} and c_{gy} represent the equivalent damping

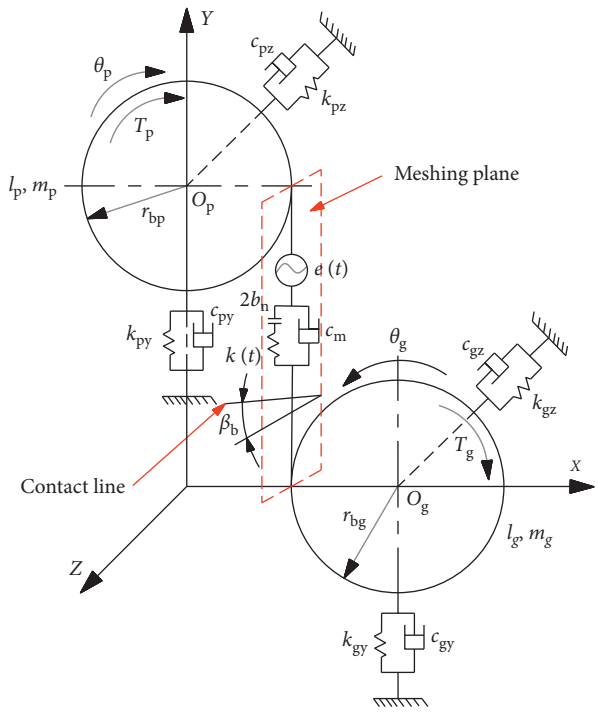

Figure 1: Bending-torsion-shaft coupling nonlinear dynamic model.

in the tangential direction; and T_p, T_g, $k(t)$, $e(t)$, c_m, $2b_n$, and β_b represent the driving torque, load torque, time-varying meshing stiffness, pitch error, meshing damping, tooth side clearance, and base circle helix angle of the helical gear pair, respectively.

2.1. Equations of Motion of the System. According to Newton's law of motion, the nonlinear dynamic equations of the system with pitch error can be obtained as follows:

$$\begin{cases} m_p\ddot{y}_p + c_{py}\dot{y}_p + k_{py}y_p = F_y, \\ m_g\ddot{y}_g + c_{gy}\dot{y}_g + k_{gy}y_g = -F_y, \\ m_p\ddot{z}_p + c_{pz}\dot{z}_p + k_{pz}z_p = -F_z, \\ m_g\ddot{z}_g + c_{gz}\dot{z}_{gp} + k_{gz}z_g = F_z, \\ I_p\ddot{\theta}_p = T_p - F_y r_{bp}, \\ I_g\ddot{\theta}_g = -T_g + F_y r_{bg}. \end{cases} \tag{1}$$

In equation (1), y_p and y_g represent the translational displacement of the driving and driven gears along the y-direction, respectively; z_p and z_g represent the translational displacement of the driving and driven gears along the z-direction, respectively; θ_p and θ_g represent the angular displacement of the driving and driven gears around the z-axis, respectively; and F_y and F_z represent the dynamic meshing force of the system along the y-direction and z-direction, respectively.

It is known that the pitch error, time-varying meshing stiffness, and meshing damping of the helical gear pair system along the meshing line direction are $k(t)$, $e(t)$, and c_m, respectively, which are decomposed into the corresponding y-direction and z-direction pitch error, time-varying meshing stiffness, and meshing damping as follows:

$$\begin{cases} e_y(t) = e(t)\cos\beta_b, \\ k_y(t) = k(t)\cos\beta_b, \\ c_{my} = c_m\cos\beta_b, \end{cases} \tag{2}$$

$$\begin{cases} e_z(t) = e(t)\sin\beta_b, \\ k_z(t) = k(t)\sin\beta_b, \\ c_{mz} = c_m\sin\beta_b. \end{cases} \tag{3}$$

According to equations (2) and (3), the relationship between the pitch error and the dynamic meshing force of the system in y and z directions is established as follows:

$$F_y = \cos\beta_b\left\{k(t)f_y\left[y_p + \theta_p r_{bp} - y_g + \theta_g r_{bg} - e_y(t)\right] + c_m\left[\dot{y}_p + \dot{\theta}_p r_{bp} - \dot{y}_g + \dot{\theta}_g r_{bg} - \dot{e}_y(t)\right]\right\}, \tag{4}$$

$$\begin{aligned} F_z = \sin\beta_b\Big\{&k(t)f_z\left[z_p - \tan\beta_b\left(\theta_p r_{bp} + y_p\right) - z_g + \tan\beta_b\left(y_g - \theta_g r_{bg}\right) - e_z(t)\right] + c_m\left[\dot{z}_p - \tan\beta_b\left(\dot{\theta}_p r_{bp} + \dot{y}_p\right)\right. \\ &\left.-\dot{z}_g + \tan\beta_b\left(\dot{y}_g - \dot{\theta}_g r_{bg}\right) - \dot{e}_z(t)\right]\Big\}. \end{aligned} \tag{5}$$

In equations (4) and (5), f_y and f_z represent the tooth side clearance functions of the system along the y-direction and z-direction, respectively.

To facilitate the calculation and analysis, equation (1) should be dimensionless. Introducing the displacement nominal scale b', make $\delta_1 = y_p/b'$, $\delta_2 = y_g/b'$, $\delta_3 = z_p/b'$, $\delta_4 = z_g/b'$, and $\delta_5 = [\theta_p r_{bp} - \theta_g r_{bg} - e(t)]/b'$. Suppose the tangential relative displacement is y_1 and the relative axial displacement is y_2 of the helical gear pair system. Define the dimensionless time as τ and the dimensionless meshing frequency as ω. y_1, y_2, τ, and ω are, respectively, as follows:

$$y_1 = \delta_1 - \delta_2 + \delta_5 - \frac{e_y(t)}{b'}, \tag{6}$$

$$y_2 = \delta_3 - \delta_4 - \tan(\delta_1 - \delta_2 + \delta_5) - \frac{e_z(t)}{b'}, \tag{7}$$

$$\tau = \omega_h t, \tag{8}$$

$$\omega = \frac{\omega_n}{\omega_h}, \tag{9}$$

$$\omega_n = 2\pi f, \tag{10}$$

$$\omega_h = \sqrt{\frac{k_m}{m_e}}, \tag{11}$$

$$m_e = \frac{I_p I_g}{\left(I_p r_g^2 + I_g r_p^2\right)}. \tag{12}$$

In equations (8)–(12), ω_h, f, k_m, and m_e are the natural frequency, meshing frequency, average meshing stiffness, and equivalent mass of the helical gear pair system, respectively.

The last two torsional dynamic equations in equation (1) are combined into a relative torsional dynamic equation, and then equation (1) is dimensionless to obtain its corresponding dimensionless nonlinear dynamic equations as follows:

$$\begin{cases} \ddot{\delta}_1 + 2\eta_{11}\dot{\delta}_1 + k_{11}\delta_1 = \cos\beta\left[k_{10}f_y(y_1) + 2\varepsilon_{10}\dot{y}_1\right], \\ \ddot{\delta}_2 + 2\eta_{21}\dot{\delta}_2 + k_{21}\delta_2 = -\cos\beta\left[k_{20}f_y(y_1) + 2\varepsilon_{20}\dot{y}_1\right], \\ \ddot{\delta}_3 + 2\eta_{12}\dot{\delta}_3 + k_{12}\delta_3 = -\sin\beta\left[k_{10}f_z(y_2) + 2\varepsilon_{10}\dot{y}_2\right], \\ \ddot{\delta}_4 + 2\eta_{22}\dot{\delta}_4 + k_{22}\delta_4 = \sin\beta\left[k_{20}f_z(y_2) + 2\varepsilon_{20}\dot{y}_2\right], \\ \ddot{\delta}_5 + \cos\beta\left[k_0 f_y(y_1) + 2\varepsilon_0\dot{y}_1\right] = f_n + \omega^2 e(\tau). \end{cases} \tag{13}$$

In equation (13), $\eta_{11} = (c_{py}/2m_p\omega_n)$; $k_{11} = (k_{py}/2m_p\omega_n^2)$; $\eta_{21} = (c_{gy}/2m_g\omega_n)$; $k_{21} = (k_{gy}/m_g\omega_n^2)$; $\eta_{12} = (c_{pz}/2m_p\omega_n)$; $k_{12} = (k_{pz}/2m_p\omega_n^2)$; $\eta_{22} = (c_{gz}/2m_g\omega_n)$; $k_{22} = (k_{gz}/m_g\omega_n^2)$; $k_{10} = (k_m/m_p\omega_n^2)$; $\varepsilon_{10} = (c_m/2m_p\omega_n)$; $k_{20} = (k_m/m_g\omega_n^2)$; $\varepsilon_{20} = (c_m/2m_g\omega_n)$; $k_0 = (k_m/m_e\omega_n^2)$; $\varepsilon_0 = (c_m/2m_e\omega_n)$; $f_n = (T_p/m_e b' r_{bp}\omega_n^2)$; and $e(\tau)$ is dimensionless pitch error, $e(\tau) = (e(\tau)/b')$.

2.2. Pitch Error. Pitch error is the difference between the actual pitch and the nominal pitch on the gear reference circle, as shown in Figure 2. Due to the presence of pitch error, the position of the gear teeth meshing will deviate from the theoretical meshing position, which causes the gear instantaneous transmission ratio change, resulting in collisions and impacts between the gear meshing tooth surfaces.

In the process of gear meshing transmission, the pitch error changes periodically with the meshing period of the gear. Therefore, this paper uses the method of simulating the pitch error as a sine function to calculate the pitch error. The pitch error is expressed as a sine function as follows:

$$e(t) = e_0 + e_r \sin(2\pi t f + \varphi). \tag{14}$$

In equation (14), e_0 is the mean of pitch error; e_r is the fluctuation amplitude of pitch error; f is gear meshing frequency; and φ is the initial phase.

The main parameters of the helical gear pair in this paper are listed in Table 1. According to the basic parameters of the helical gear pair in Table 1, the relevant error values of the helical gear pair are obtained by checking GB/T 10095.1-2008. In addition, make $e_0 = 0$ and $\varphi = 0$ and get the simulation curve of pitch error in a meshing cycle of this helical gear pair as shown in Figure 3.

The above calculation results are basically consistent with the experimental measurement results of the pitch error in reference [40], thus verifying the correctness of the method used.

2.3. Calculation of Time-Varying Meshing Stiffness. The contact ratio of helical gear is generally greater than 2. In the process of gear meshing, $N(N \geq 1)$ pairs of teeth and $N+1$ pairs of teeth are engaged alternately, making the meshing stiffness of the gear also change continuously and periodically, i.e., time-varying meshing stiffness. The meshing process of gear is assumed to be composed of many momentarily varying meshing contact lines, and the elastic deformation of the gear teeth is obtained by calculating the total length of the contact lines. On this basis, the time-varying meshing stiffness of the gear is determined.

For the helical gear pair studied in this paper, the contact ratio is 2.7573. According to the relationship of the contact ratio, the formula for calculating the total contact line length $l(t)$ in one meshing period of the helical gear pair is deduced as follows:

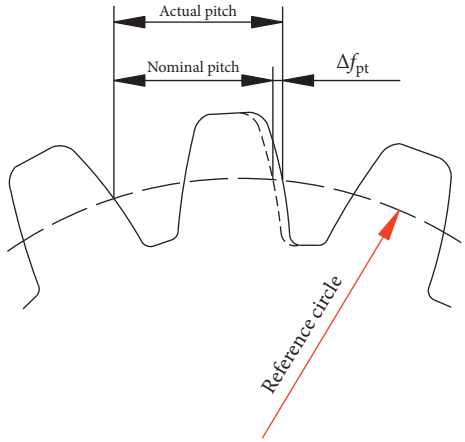

Figure 2: Pitch error.

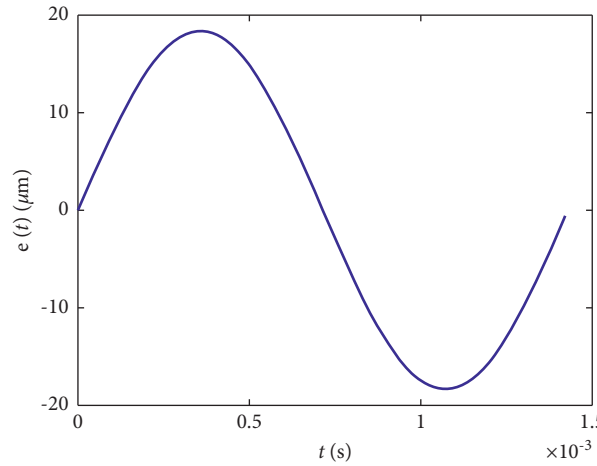

Figure 3: Simulation curve of pitch error.

Table 1: Main parameters of helical gear pair.

Parameter	Driving gear	Driven gear
Number of teeth z	21	38
Module m_n (mm)	2.166	
Pressure angle α_n (°)	20	
Helix angle β (°)	20	−20
Contact ratio ε_γ	2.7573	
Face width B (mm)	15	
Rotational speed n (rpm)	2000	1105.26
Accuracy/level	7	7
Material	45	45

$$l(t) = \begin{cases} 2l_{\max} + \dfrac{l_{\max}}{t_1} t, & 0 \le t < t_2 - 2t_z, \\ 2l_{\max} + \dfrac{l_{\max}}{t_1} (t_2 - 2t_z), & t_2 - 2t_z \le t < t_1, \\ 2l_{\max} + \dfrac{l_{\max}}{t_1} (t_1 + t_2 - 2t_z - t), & t_1 \le t < t_1 + t_2 - 2t_z, \\ 2l_{\max}, & t_1 + t_2 - 2t_z \le t \le t_z. \end{cases} \tag{15}$$

In equation (15), $l_{\max}$ is the maximum contact line length in one meshing cycle and t_z is the meshing period of the gear pair; its calculation equations are, respectively, as follows:

$$l_{\max} = \frac{B}{\cos \beta_b}, \qquad t_z = \frac{60}{n_1 z_1}. \tag{16}$$

Therefore, the time-varying meshing stiffness $k(t)$ can be obtained as follows [41]:

$$k(t) = \lambda \cdot l(t), \tag{17}$$

where λ is as follows:

$$\lambda = \frac{k_m}{l_m}. \tag{18}$$

In equation (18), λ is the conversion factor between meshing stiffness and contact line length; k_m is the average meshing stiffness; and l_m is the average value of the total contact line length in a meshing period.

Combining the data in Table 1, the average meshing stiffness of this helical gear pair is calculated to be 13.3548 N/(μm•mm) according to the relevant formulas in GB/T 3480.1-2019. On this basis, the time-varying meshing stiffness of the helical gear pair is obtained. In order to facilitate subsequent calculations, this paper uses a 6-order Fourier series to fit the time-varying meshing stiffness to get the following equation:

$$k(t) = k_m + \sum_{n=1}^{6} \left[a_n \cos\left(\frac{2\pi n}{t_z} t\right) + c_n \sin\left(\frac{2\pi n}{t_z} t\right) \right]. \tag{19}$$

In equation (19), a_n and c_n are Fourier series coefficients, and the specific values of the Fourier series coefficients are shown in Table 2. The corresponding fitted curve is shown in Figure 4.

2.4. Meshing Damping. The meshing damping is mainly related to the meshing damping ratio, average meshing stiffness, and mass of the gear. The meshing damping of the gear can be calculated by the following equation [1]:

$$c_m = 2\xi \sqrt{\frac{k_m r_{bp}^2 r_{bg}^2 I_p I_g}{r_{bp}^2 I_p + r_{bg}^2 I_g}}. \tag{20}$$

In equation (20), ξ is the damping ratio, which usually takes the value range of [0.03, 0.17] and is taken as 0.1 in this paper; k_m is the average meshing stiffness; r_{bp} and r_{bg} are the base circle radius of the driving and driven gears, respectively; and I_p and I_g are the moments of inertia of the driving and driven gears, respectively.

Table 2: Fourier series coefficients of time-varying meshing stiffness.

Coefficient code	Corresponding value	Coefficient code	Corresponding value
a_1	−1.202	c_1	1.203
a_2	$-5.79e-5$	c_2	$-1.15e-4$
a_3	−0.1339	c_3	−0.1335
a_4	$-5.784e-5$	c_4	$9.478e-8$
a_5	−0.04809	c_5	0.04819
a_6	$-5.79e-5$	c_6	$-3.819e-5$

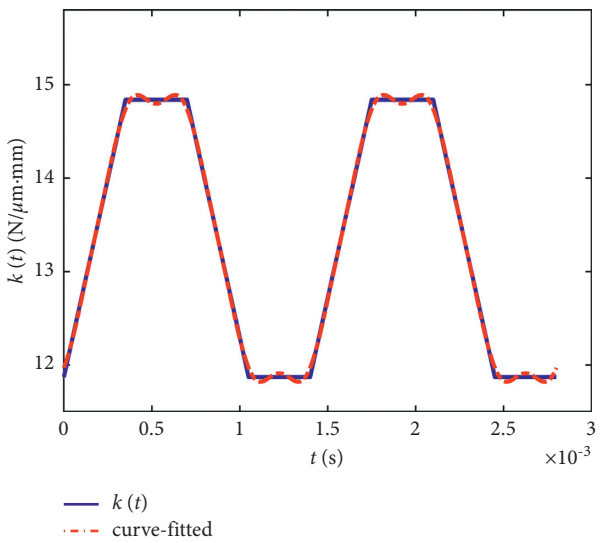

Figure 4: Fourier series fitting curve of time-varying meshing stiffness.

According to the main parameters of the helical gear pair in Table 1, the relevant values are substituted into equation (20). By calculation, the value of the meshing damping of this helical gear pair can be obtained as follows:

$$c_m = 247.331 \frac{\mathrm{N}}{\mathrm{m} \cdot \mathrm{s}^{-1}}. \tag{21}$$

2.5. Tooth Side Clearance. To facilitate the storage of lubricating oil and prevent the tooth surface from being stuck by thermal expansion, gear in the assembly process along the direction of the meshing line to leave a specific tooth side clearance. The tooth side clearance function can be expressed as follows [12]:

$$f(x(t)) = \begin{cases} x(t) - b_n, & (x(t) > b_n), \\ 0, & (|x(t)| \le b_n), \\ x(t) + b_n, & (x(t) < -b_n). \end{cases} \tag{22}$$

In equation (22), b_n is the half tooth side clearance.

The corresponding y-direction and z-direction tooth side clearance functions of the helical gear pair system in this paper can be obtained as follows:

$$f_y(x(t)) = \begin{cases} x(t) - b_n \cos\beta_b, & x(t) > b_n \cos\beta_b, \\ 0, & |x(t)| \le b_n \cos\beta_b, \\ x(t) + b_n \cos\beta_b, & x(t) < -b_n \cos\beta_b, \end{cases}$$
$$f_z(x(t)) = \begin{cases} x(t) - b_n \sin\beta_b, & x(t) > b_n \sin\beta_b, \\ 0, & |x(t)| \le b_n \sin\beta_b, \\ x(t) + b_n \sin\beta_b & x(t) < -b_n \sin\beta_b. \end{cases} \tag{23}$$

3. Numerical Results and Discussion

3.1. Analysis of System Vibration Characteristics with and without Pitch Error. According to whether the pitch error is added to the nonlinear dynamic equations of the system, the system equations are solved, and the vibration acceleration time-domain curves of the system in each degree of freedom direction with and without pitch error are obtained as shown in Figure 5.

It can be seen from Figure 5 that

(1) Since the system operates at 2000 rpm, its dimensionless meshing frequency is calculated to be 0.1394 and the corresponding dimensionless meshing period is 7.1736. From Figure 5, it can be seen that the vibration acceleration response of the system in each direction has apparent periodicity and the corresponding period is very close to the dimensionless meshing period, so the accuracy of the calculation results can be confirmed from this perspective.

(2) The changing trend of the time-domain curves of vibration acceleration in each direction after adding the pitch error is basically the same as the changing trend of the time-domain curves of vibration acceleration in each direction without adding the pitch error, still showing obvious periodicity, but the phase changes to a certain extent. In addition, the amplitudes of vibration acceleration in each direction increase slightly after adding the pitch error.

(3) The amplitudes of vibration acceleration in the torsional direction of the system are much greater than those in the tangential and axial directions. This shows that torsional vibration is the primary vibration form of the system, while tangential and axial

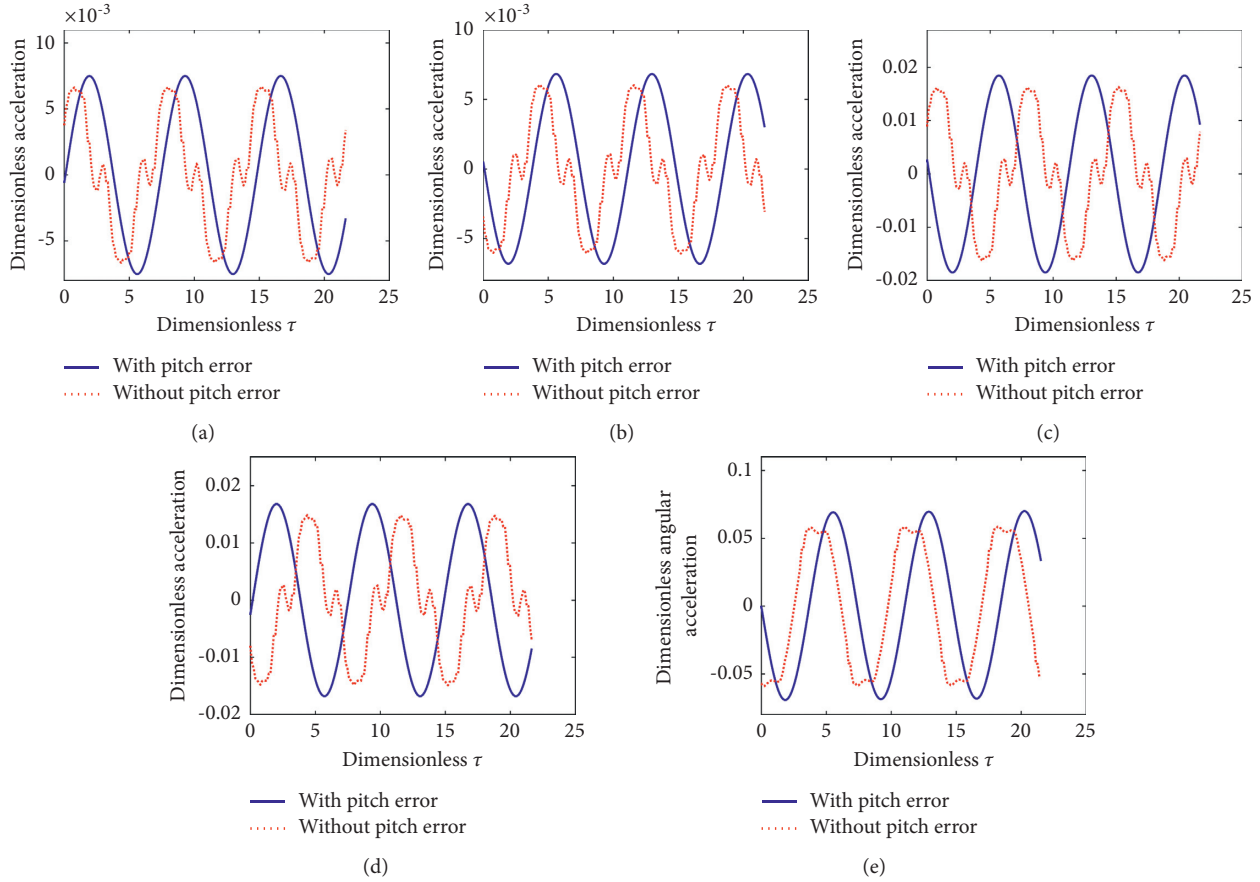

Figure 5: The time-domain curves of vibration acceleration of the helical gear pair system with and without pitch error: (a) tangential vibration acceleration of driving gear; (b) tangential vibration acceleration of driven gear; (c) axial vibration acceleration of driving gear; (d) axial vibration acceleration of driven gear; (e) vibration acceleration in the torsional direction.

vibration can be considered as a coupling vibration generated by torsional vibration as the excitation force.

(4) The variations of vibration acceleration amplitude in each direction of the system after adding pitch error are shown in Table 3. It can be seen from Table 3 that the maximum change degree of vibration acceleration amplitude in each direction after pitch error is in the torsional direction, followed by the axial direction, and the minimum change degree is in the tangential direction. This indicates that the pitch error has the most significant influence on the torsional direction of this helical gear system, followed by the axial direction and the least tangential direction.

To further study the characteristics of the system vibration response with and without pitch error, the fast Fourier transform (FFT) can be done for the time-domain response of the vibration acceleration in each direction to analyze its frequency domain characteristics. The vibration acceleration spectrum maps of the system in the direction of each degree of freedom are shown in Figure 6.

It can be seen from Figure 6 that

(1) The main frequency components of the vibration acceleration response of the system in each direction with and without pitch error are all the dimensionless meshing frequency (0.1394). Therefore, in order to prevent the resonance of the system, the overlap between the meshing frequency and the system's natural frequency should be avoided in the system operation process.

(2) From the perspective analysis of the magnitude of the acceleration amplitude change, the conclusion obtained is consistent with the analysis result of the vibration acceleration in the time domain: after adding the pitch error, the amplitudes of the vibration acceleration vary the extent the most in the torsional direction, followed by the axial direction, and the degree of tangential direction variation is minimal.

Through the analysis of Figures 5 and 6, it can be seen that the vibration in the torsional direction of the system is the dominant vibration, and the degree of influence on the torsional orientation of the system after adding the pitch error is the greatest, followed by the axial direction, and the tangential direction is the least.

Table 3: Variations of vibration acceleration amplitude in each degree of freedom direction of the helical gear pair system after adding pitch error.

	Tangential direction		Axial direction		Torsional direction
	Driving gear	Driven gear	Driving gear	Driven gear	
Variation of vibration acceleration amplitude	0.0009	0.0007	0.0022	0.0019	0.0113

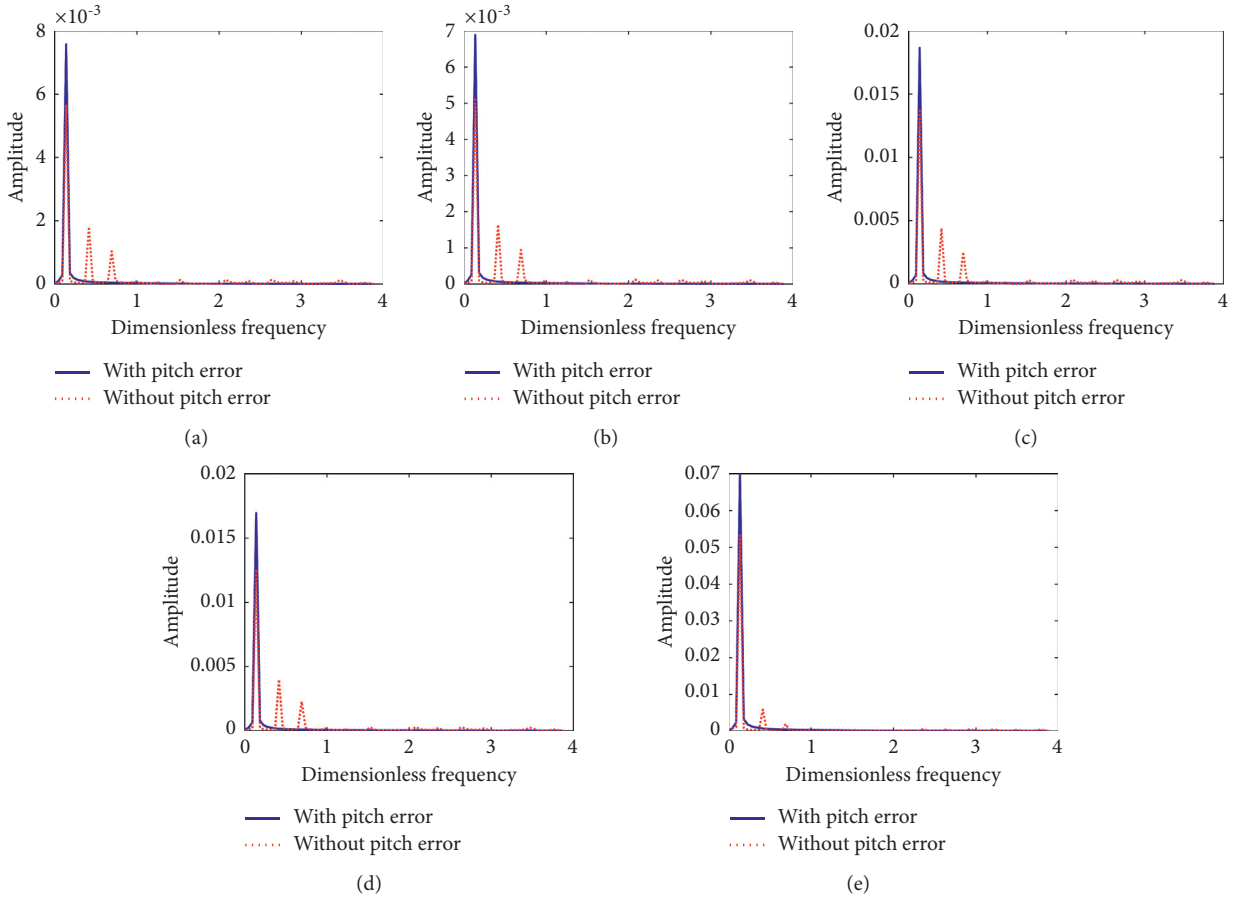

Figure 6: Vibration acceleration spectrum maps of the helical gear pair system with and without pitch error: (a) tangential vibration acceleration of driving gear; (b) tangential vibration acceleration of driven gear; (c) axial vibration acceleration of driving gear; (d) axial vibration acceleration of driven gear; (e) vibration acceleration in the torsional direction.

3.2. Influence of Pitch Error on Bifurcation and Chaos Characteristics of the System. From the analysis in Section 3.1, it can be seen that the introduction of pitch error has a much more significant impact on the torsional direction of the helical gear pair system than on the tangential and axial directions. Therefore, this section mainly investigates the effect on the bifurcation and chaos characteristics of the helical gear pair system in the torsional direction when the pitch error varies numerically.

When the pitch error takes the values of $[0e(\tau), 15e(\tau)]$ and other parameters are kept constant, the system equations are solved. The bifurcation diagram of the relative torsional displacement of the system with the variation of pitch error is obtained as shown in Figure 7(a), and the corresponding LLE chart is shown in Figure 7(b).

As shown in Figure 7, with the increase in pitch error, the motion state of the system undergoes six stages of change: one time periodic motion→two times periodic motion→ quasi-periodic motion→chaotic motion→three times periodic motion→chaotic motion. When the pitch error $\in [0e(\tau), 10.07e(\tau)]$, the system is in one time-periodic motion state, and the corresponding LLE is less than 0. When the pitch error $\in [10.08e(\tau), 11.16e(\tau)]$, the system undergoes a doubling bifurcation, bifurcating from one time-periodic motion state to two times periodic motion state, and the corresponding LLE is less than 0. When the pitch error $\in [11.17e(\tau), 11.77e(\tau)]$, the system enters a short quasiperiodic motion state; at this time, the LLE becomes 0. When the pitch error $\in [11.78e(\tau), 12.82e(\tau)]$, the system enters an unstable, chaotic motion state, and the corresponding LLE is greater than 0. After a short period of chaotic motion, when the pitch error $\in [12.83e(\tau), 13.04e(\tau)]$, the

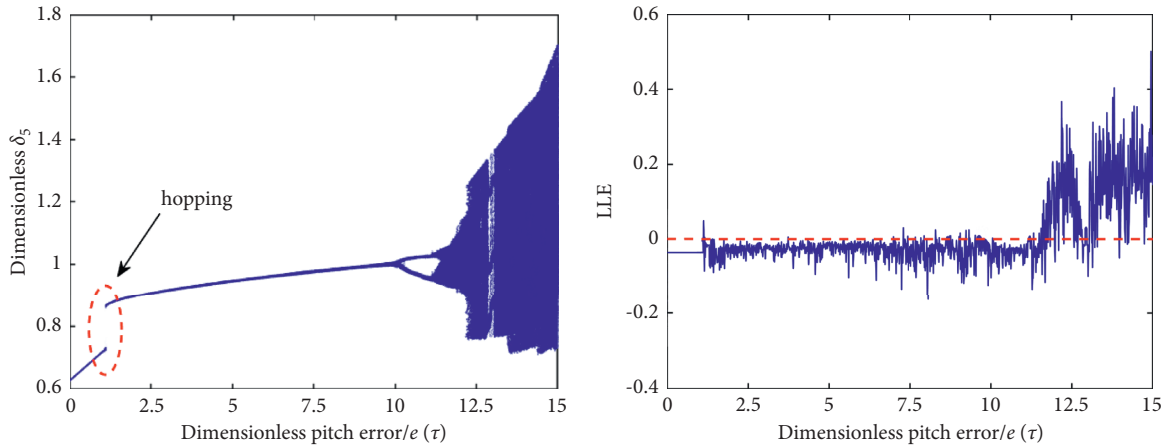

Figure 7: (a) Bifurcation diagram. (b) LLE chart.

system enters a short period of three times periodic motion state again, and the corresponding LLE is less than 0. Finally, the system stays in an unstable and complexly changing state, namely, chaotic motion state, and the corresponding LLE is greater than 0. Moreover, the phenomenon of pitch error hopping occurs at the point of $1.12e(\tau)$, where the LLE is −0.0043. Such sudden transition is named as a discontinuous bifurcation (marked by hopping in Figure 7(a)). This hopping occurs for some bifurcation parameter values for which the nonlinear dynamics can be either periodic or chaotic. In Figure 7(a), the hopping induces a transition from periodic gait to periodic gait.

The above is a global analysis of the movement characteristics of the entire helical gear pair system with the change of pitch error. In order to verify whether the system motion state described in Figure 7 is correct, the following local analysis is used to further investigate the motion characteristics of the system at some special stages.

When the pitch error takes different values, the corresponding time-domain diagrams, phase diagrams, and Poincaré cross-section graphs are obtained as shown in Figures 8–13.

As shown in Figures 8, 9, and 12, when the pitch error takes the values of $5.86e(\tau)$, $10.75e(\tau)$, and $12.97e(\tau)$, the corresponding time-domain diagrams have apparent periodicity, the phase diagrams are a closed curve, and the Poincaré cross-section graphs consist of a finite number of points, so the system is in a periodic motion state at this time. And because the phase diagram corresponding to Figure 8 is a closed curve and the Poincaré cross-section graph is a point, the phase diagram corresponding to Figure 9 is two closed curves, and the Poincaré cross-section graph is two discrete points; the phase diagram corresponding to Figure 12 is three closed curves, and the Poincaré cross-section graph is three discrete points, so the specific motion states of the system at this time are one time, two times, and three times periodic motion states, respectively. As shown in Figure 10, when the pitch error takes the value of $11.64e(\tau)$, its corresponding time-domain diagram has a certain periodicity, the phase diagram is two closed bands of curves, and the Poincaré cross-section graph consists of a finite set of points, and the number of point sets is two, so the system is in a two times quasiperiodic motion state at this time. As shown in Figures 11 and 13, when the pitch error is taken as $12.47e(\tau)$ and $14.68e(\tau)$, the corresponding time-domain diagrams have no apparent periodicity, the phase diagrams are irregular and fill a closed area, and the Poincaré cross-section graphs consist of patches of dense points, so the system is in a chaotic motion state at this time.

From the above local analysis, it can be seen that the motion states of the system during the special phase are consistent with the results of the global analysis, thus verifying the correctness of the global analysis.

The global and local analysis shows that when the pitch error $\in [0e(\tau), 10.07e(\tau)]$, $[10.08e(\tau), 11.16e(\tau)]$, and $[12.83e(\tau), 13.04e(\tau)]$, the system is in one time, two times, and three times periodic motion state, respectively, which is the ideal working region of the system. At this time, the system's movement is more stable, and the vibration noise is small.

3.3. Impact of Pitch Error on the Vibration Characteristics of the System. The analysis of Section 3.2 shows that the system is in a periodic motion state when the pitch error $\in [0e(\tau), 11.16e(\tau)]$. Therefore, this section mainly studies the effect on the vibration characteristics of the system in the torsional direction when the pitch error varies by the same degree in the cyclic motion state.

The pitch errors of $e(\tau)$, $3e(\tau)$, $5e(\tau)$, $7e(\tau)$, $9e(\tau)$, and $11e(\tau)$ are taken into the system equations, respectively, and the other parameters remain unchanged. The system equations are solved to obtain the time-domain curves of vibration acceleration in the torsional direction of the system corresponding to different pitch errors, as shown in Figure 14.

It can be seen from Figure 14 that

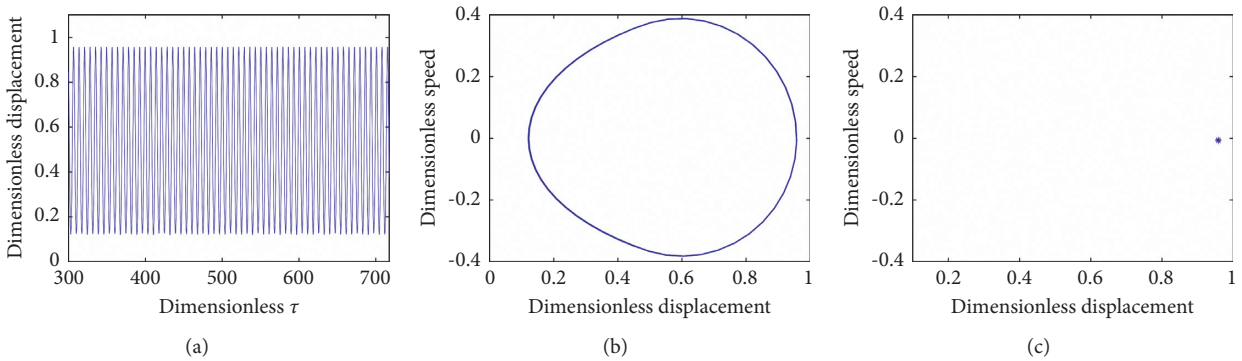

Figure 8: Pitch error = $5.86e(\tau)$. (a) Time-domain diagram. (b) Phase diagram. (c) Poincaré cross-section graph.

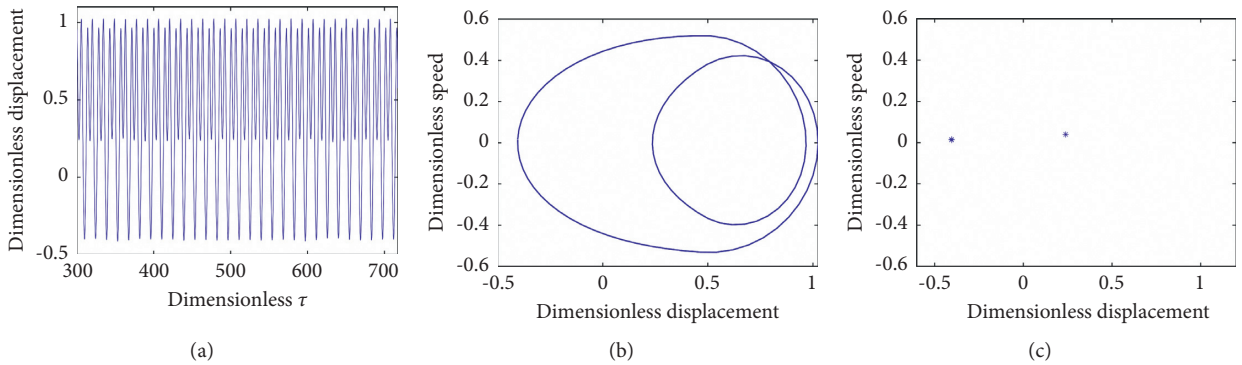

Figure 9: Pitch error = $10.75e(\tau)$. (a) Time-domain diagram. (b) Phase diagram. (c) Poincaré cross-section graph.

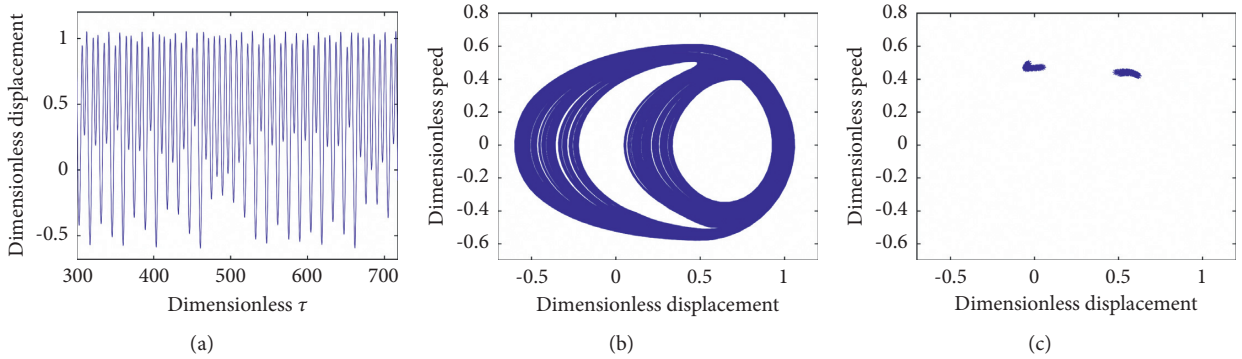

Figure 10: Pitch error = $11.64e(\tau)$. (a) Time-domain diagram. (b) Phase diagram. (c) Poincaré cross-section graph.

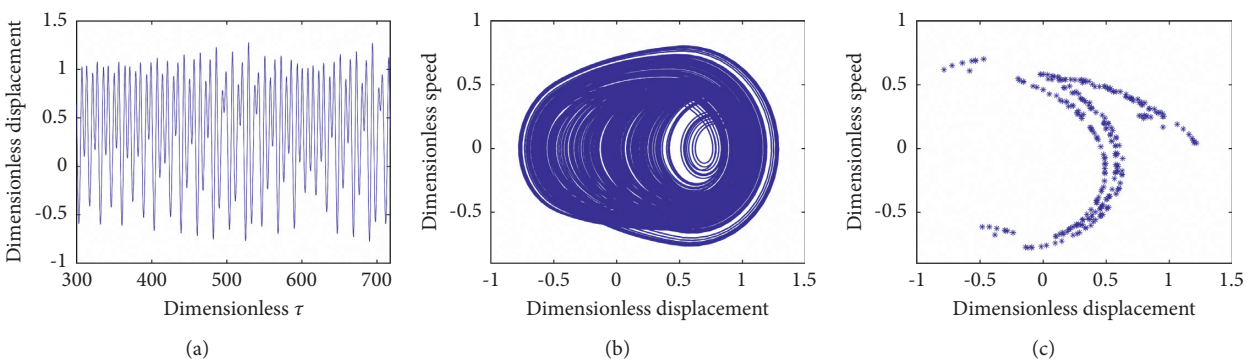

Figure 11: Pitch error = $12.47e(\tau)$. (a) Time-domain diagram. (b) Phase diagram. (c) Poincaré cross-section graph.

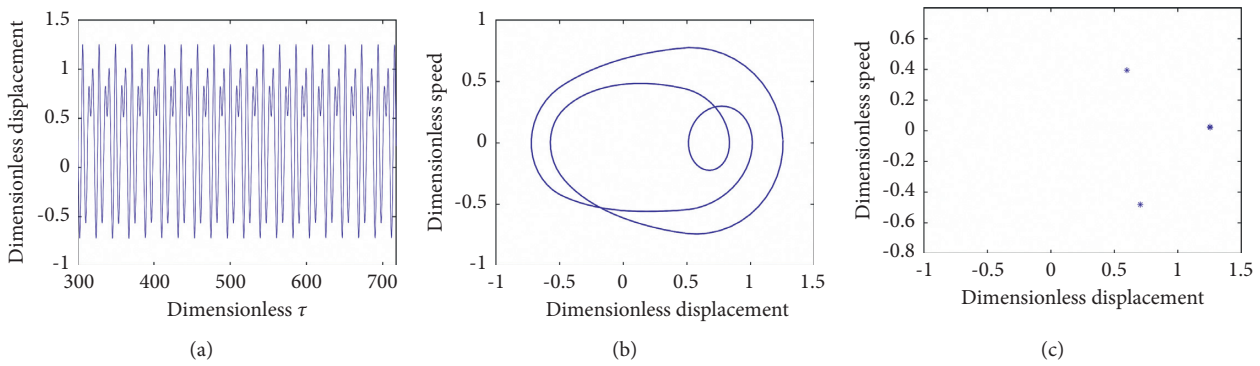

Figure 12: Pitch error = $12.97e(\tau)$. (a) Time-domain diagram. (b) Phase diagram. Poincaré cross-section graph.

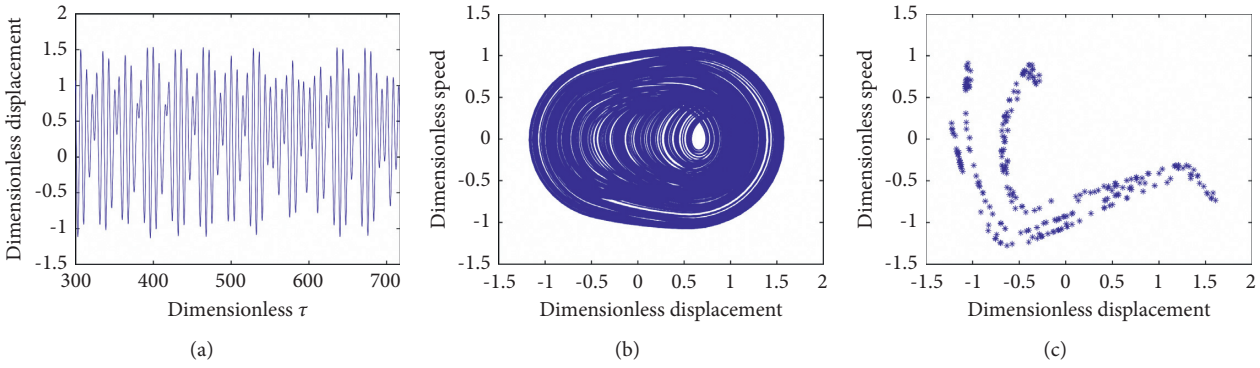

Figure 13: Pitch error = $14.68e(\tau)$. (a) Time-domain diagram. (b) Phase diagram. (c) Poincaré cross-section graph.

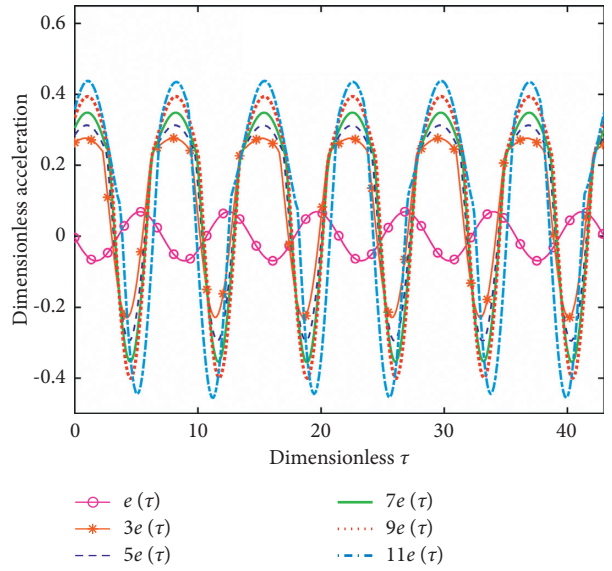

Figure 14: Time-domain curves of vibration acceleration in the torsional direction of the system with different pitch errors.

(1) When the value of pitch error increases, the corresponding amplitude of vibration acceleration also increases accordingly.

(2) When the pitch error changes from $e(\tau)$ to $3e(\tau)$, $3e(\tau)$ to $5e(\tau)$, $5e(\tau)$ to $7e(\tau)$, $7e(\tau)$ to $9e(\tau)$, and $9e(\tau)$ to $11e(\tau)$, their corresponding vibration acceleration amplitude changes are 0.2163, 0.0354, 0.0359, 0.0356, and 0.0357, respectively. It can be seen that when the pitch error changes from $e(\tau)$ to $3e(\tau)$, the corresponding vibration acceleration amplitude changes significantly more than in the other cases. The main reason is that the pitch error causes the jump

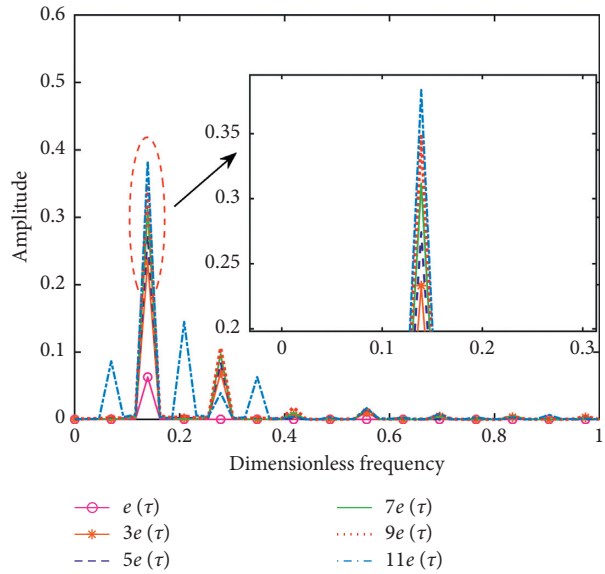

Figure 15: Vibration acceleration spectrum map of the system in the torsional direction at different pitch errors.

phenomenon when the pitch error changes from $e(\tau)$ to $3e(\tau)$.

(3) When the pitch error varies by the same degree ($2e(\tau)$) and there is no jump phenomenon in the process of pitch error variation, the system will produce a certain vibration response change in the torsional direction.

To further study the characteristics of the system torsional direction vibration response when the pitch error changes, the FFT is done on the time-domain response of the system torsional direction vibration acceleration, and the spectrum map of the system torsional direction vibration acceleration at different pitch errors is obtained as shown in Figure 15.

It can be seen from Figure 15 that

(1) The main frequency components of the vibration acceleration response of the system in the torsional direction for different pitch errors are all dimensionless meshing frequencies (0.1394).

(2) From the perspective analysis of acceleration response amplitude change, the conclusion obtained is consistent with the result of vibration acceleration in the time-domain analysis: when the pitch error varies by the same degree ($2e(\tau)$) and there is no jump phenomenon in the process of pitch error variation, it will produce a certain impact on the torsional direction vibration response of the system.

Through the analysis of Figures 14 and 15, it can be seen that when the system is in a periodic motion state, the pitch error changes to the same degree ($2e(\tau)$) and there is no jump phenomenon during the change of pitch error, and the system will produce a specific vibration response change in the torsional direction, i.e., the increased or decreased degree of the vibration response in the torsional orientation of the system caused by the change of the pitch error by the same degree each time is almost the same.

4. Conclusions and Future Works

In this paper, a bending-torsion-shaft coupling nonlinear dynamic model of the helical gear pair system is established considering the effect of pitch error. The pitch error is calculated by using the method of simulating the pitch error as a sine function. Then, the motion equations of the system are solved by the Runge–Kutta numerical integration method. The effect of pitch error on the vibration, bifurcation, and chaos characteristics of the system is investigated in detail.

The major conclusions can be summarized as follows:

(1) The introduction of pitch error has the greatest degree of effect on the vibration acceleration response of the helical gear pair system in the torsional direction, followed by the axial direction and the smallest in the tangential direction.

(2) With the increase in pitch error, the helical gear pair system shows complex motion characteristics in the torsional direction. Its motion state undergoes six stages of changes: one time-periodic motion, two times periodic motion, quasiperiodic motion, chaotic motion, three times periodic motion, and chaotic motion. Ultimately the system stays in an unstable and complexly changing chaotic motion state.

(3) Under the condition that the helical gear pair system is in a periodic motion state when the pitch error varies to the same extent and there is no jump phenomenon in the process of pitch error variation, the system will produce a certain change in vibration response in the torsional direction.

Based on the conclusions of the work, the following can be further explored:

(1) We investigated the nonlinear dynamic characteristics of the six degrees of freedom helical gear pair system in the present work. As a future direction, our methodology introduced in the current work can be extended to analyze nonlinear dynamic characteristics of helical gear pair systems with more degrees of freedom.

(2) Based on the optimal control principle, a reasonable control strategy can be proposed, and then the corresponding controller can be designed to realize the smooth operation of the gear system.

Data Availability

The data used to support the findings of this study are available from the corresponding author upon request.

Conflicts of Interest

The authors declare that there are no conflicts of interest regarding the publication of this paper.

Acknowledgments

The authors gratefully acknowledge the financial support from the National Natural Science Foundation of China (grant no. 51965037). This work was supported by the National Natural Science Foundation of China (grant no. 51965037).

References

[1] J. Yang, R. Sun, D. Yao, J. Wang, and C. Liu, "Nonlinear dynamic analysis of high speed multiple units gear transmission system with wear fault," *Mechanical Sciences*, vol. 10, no. 1, pp. 187–197, 2019.

[2] Q. Tian, P. Flores, and H. M. Lankarani, "A comprehensive survey of the analytical, numerical and experimental methodologies for dynamics of multibody mechanical systems with clearance or imperfect joints," *Mechanism and Machine Theory*, vol. 122, pp. 1–57, 2018.

[3] S. Rahmanian and M. R. Ghazavi, "Bifurcation in planar slider-crank mechanism with revolute clearance joint," *Mechanism and Machine Theory*, vol. 91, pp. 86–101, 2015.

[4] Q. Wang, Z. Li, H. Ma, and B. Wen, "Effects of different coupling models of a helical gear system on vibration characteristics," *Journal of Mechanical Science and Technology*, vol. 31, no. 5, pp. 2143–2154, 2017.

[5] C. Wang, "Dynamic model of a helical gear pair considering tooth surface friction," *Journal of Vibration and Control*, vol. 26, no. 15-16, pp. 1356–1366, 2020.

[6] H. Jiang, Y. Shao, C. K. Mechefske, and X. Chen, "The influence of mesh misalignment on the dynamic characteristics of helical gears including sliding friction," *Journal of Mechanical Science and Technology*, vol. 29, no. 11, pp. 4563–4573, 2015.

[7] F. Wang, Z. D. Fang, and S. J. Li, "Nonlinear dynamic analysis of helical gear considering meshing impact," *Applied Mechanics and Materials*, vol. 201-202, pp. 135–138, 2012.

[8] B. S. Yan, R. Y. Li, and C. H. Liu, "Dynamic analysis on the bend-torsion-shaft-pendulum coupling vibration model of helical gear," *Applied Mechanics and Materials*, vol. 851, pp. 273–278, 2016.

[9] Y. Zhang, Q. Wang, H. Ma, J. Huang, and C. Zhao, "Dynamic analysis of three-dimensional helical geared rotor system with geometric eccentricity," *Journal of Mechanical Science and Technology*, vol. 27, no. 11, pp. 3231–3242, 2013.

[10] W. Yu, C. K. Mechefske, and M. Timusk, "The dynamic coupling behaviour of a cylindrical geared rotor system subjected to gear eccentricities," *Mechanism and Machine Theory*, vol. 107, pp. 105–122, 2017.

[11] L. Han and H. Qi, "Dynamics responses analysis in frequency domain of helical gear pair under multi-fault conditions," *Journal of Mechanical Science and Technology*, vol. 33, no. 11, pp. 5117–5127, 2019.

[12] K. Huang, Y. Yi, Y. S. Xiong, Z. B. Cheng, and H. Chen, "Nonlinear dynamics analysis of high contact ratio gears system with multiple clearances," *Journal of the Brazilian Society of Mechanical Sciences and Engineering*, vol. 42, no. 4, pp. 69–76, 2020.

[13] R. L. Zhang, K. D. Wang, Y. D. Shi, X. Sun, F. Gu, and T. Wang, "The influences of gradual wears and bearing clearance of gear transmission on dynamic responses," *Energies*, vol. 12, no. 24, Article ID 4731, 2019.

[14] R. Xu, J. Zhang, J. G. Wang, R. J. Li, and K. Huang, "Nonlinear dynamic modelling and analysis for a spur gear pair considering tooth profile deviation based on tooth contact analysis," *Journal of Vibration Engineering & Technologies*, vol. 9, no. 6, pp. 1–19, 2021.

[15] G. Arian and S. Taghvaei, "Dynamic analysis and chaos control of spur gear transmission system with idler," *European Journal of Mechanics-A: Solids*, vol. 87, no. 1, Article ID 104229, 2021.

[16] A. Saghafi and A. Farshidianfar, "An analytical study of controlling chaotic dynamics in a spur gear system," *Mechanism and Machine Theory*, vol. 96, pp. 179–191, 2016.

[17] X. Hua and Z. G. Chen, "Effect of roller bearing elasticity on spiral bevel gear dynamics," *Advances in Mechanical Engineering*, vol. 12, no. 7, pp. 1–9, 2020.

[18] M. H. Yin, Y. H. Cui, X. J. Meng, J. Z. Zuo, and Y. H. Qi, "Dynamic analysis of double-helical gear system considering effect of oil film among meshing teeth," *Advances in Mechanical Engineering*, vol. 12, no. 5, pp. 1–14, 2020.

[19] G. F. Li, S. P. Wu, H. B. Wang, and W. C. Ding, "Global dynamics of a non-smooth system with elastic and rigid impacts and dry friction," *Communications in Nonlinear Science and Numerical Simulation*, vol. 95, no. 2, Article ID 105603, 2021.

[20] O. Makarenkov and J. S. W. Lamb, "Dynamics and bifurcations of nonsmooth systems: a survey," *Physica D: Nonlinear Phenomena*, vol. 241, no. 22, pp. 1826–1844, 2012.

[21] H. Gritli and S. Belghith, "Diversity in the nonlinear dynamic behavior of a one-degree-of-freedom impact mechanical oscillator under OGY-based state-feedback control law: order, chaos and exhibition of the border-collision bifurcation," *Mechanism and Machine Theory*, vol. 124, pp. 1–41, 2018.

[22] H. Gritli and S. Belghith, "Displayed phenomena in the semi-passive torso-driven biped model under OGY-based control method: birth of a torus bifurcation," *Applied Mathematical Modelling*, vol. 40, no. 4, pp. 2946–2967, 2016.

[23] K. Umezawa, T. Sato, and K. Kohno, "Influence of gear errors on rotational vibration of power transmission spur gears: 1st report, pressure angle error and normal pitch error," *Bulletin of JSME*, vol. 27, no. 225, pp. 569–575, 1984.

[24] K. Umezawa and T. Sato, "Influence of gear error on rotational vibration of power transmission spur gear: 3rd report, accumulative pitch error," *Bulletin of JSME*, vol. 28, no. 246, pp. 3018–3024, 1985.

[25] P. F. Liu, L. Y. Zhu, X. F. Gou, J. F. Shi, and G. G. Jin, "Modeling and analyzing of nonlinear dynamics for spur gear pair with pitch deviation under multi-state meshing," *Mechanism and Machine Theory*, vol. 163, no. 3, Article ID 104378, 2021.

[26] M. J. Handschuh, A. Kahraman, and M. R. Milliren, "Impact of tooth spacing errors on the root stresses of spur gear pairs," *Journal of Mechanical Design*, vol. 136, no. 6, Article ID 061010, 2014.

[27] M. Inalpolat, M. Handschuh, and A. Kahraman, "Influence of indexing errors on dynamic response of spur gear pairs," *Mechanical Systems and Signal Processing*, vol. 60-61, pp. 391–405, 2015.

[28] D. Talbot, A. Sun, and A. Kahraman, "Impact of tooth indexing errors on dynamic factors of spur gears: experiments and model simulations," *Journal of Mechanical Design*, vol. 138, no. 9, Article ID 093302, 2016.

[29] P. Velex, M. Maatar, and J.-P. Raclot, "Some numerical methods for the simulation of geared transmission dynamic behavior formulation and assessment," *Journal of Mechanical Design*, vol. 119, no. 2, pp. 292–298, 1997.

[30] M. Franulovic, K. Markovic, Z. Vrcan, and M. Soban, "Experimental and analytical investigation of the influence of pitch deviations on the loading capacity of HCR spur gears," *Mechanism and Machine Theory*, vol. 117, pp. 96–113, 2017.

[31] L. Walha, T. Fakhfakh, and M. Haddar, "Nonlinear dynamics of a two-stage gear system with mesh stiffness fluctuation, bearing flexibility and backlash," *Mechanism and Machine Theory*, vol. 44, no. 5, pp. 1058–1069, 2009.

[32] A. Al-shyyab and A. Kahraman, "Non-linear dynamic analysis of a multi-mesh gear train using multi-term harmonic balance method: sub-harmonic motions," *Journal of Sound and Vibration*, vol. 279, no. 1, pp. 417–451, 2003.

[33] A. Al-shyyab and A. Kahraman, "Non-linear dynamic analysis of a multi-mesh gear train using multi-term harmonic balance method: period-one motions," *Journal of Sound and Vibration*, vol. 284, no. 1, pp. 151–172, 2004.

[34] S. Y. Chen and J. Y. Tang, "Effects of staggering and pitch error on the dynamic response of a double-helical gear set," *Journal of Vibration and Control*, vol. 23, no. 11, pp. 1844–1856, 2017.

[35] F. Wang, X. Xu, Z. D. Fang, and L. Chen, "Study of the influence mechanism of pitch deviation on cylindrical helical gear meshing stiffness and vibration noise," *Advances in Mechanical Engineering*, vol. 9, no. 9, pp. 810–818, 2017.

[36] B. Yuan, G. Liu, and L. Liu, "Quasi-static characteristics and vibration responses analysis of helical geared rotor system with random cumulative pitch deviations," *Applied Sciences*, vol. 10, no. 12, Article ID 4403, 2020.

[37] B. Yuan, S. Chang, G. Liu, and L. Y. Wu, "Quasi-static and dynamic behaviors of helical gear system with manufacturing errors," *Chinese Journal of Mechanical Engineering*, vol. 31, no. 1, pp. 1–9, 2018.

[38] F. Guo and Z.-D. Fang, "A new algorithm to solve meshing-in impact considering the measured pitch error and to investigate its influence on the dynamic characteristics of a gear system," *International Journal of Precision Engineering and Manufacturing*, vol. 20, no. 3, pp. 395–406, 2019.

[39] S. S. Rao, *Mechanical Vibrations*, Pearson Education Limited, New York, NY, USA, 2017.

[40] S. Yang, *Research on Experiment Comparison about Two Measuring Methods of Gears Pitch Deviation*, Xi'an Technological University, Xi'an, China, 2018.

[41] Q. Zhang, *Dynamics Characteristics Analysis and Experimental Study of a Gearbox*, Chongqing University, Chongqing, China, 2014.